Med Chem Res
DOI 10.1007/s00044-012-0428-9

MEDICINAL CHEMISTRY RESEARCH

ORIGINAL RESEARCH

Structure–activity relationship investigation of methoxy substitution on anticancer pyrimido[4,5-c]quinolin-1(2*H*)-ones

Kamel Metwally · Ashraf Khalil · Asmaa Sallam · Harris Pratsinis · Dimitris Kletsas · Khalid El Sayed

Received: 26 March 2012 / Accepted: 15 December 2012

Abstract Pyrimido[4,5-c]quinolin-1(2*H*)-one derivatives were shown to exert interesting biological activities including anticancer, antimicrobial, and cardiovascular. Substitution with methoxy groups played a crucial role in the anticancer activity of known anticancer agents. This study explores the contribution of diverse-positioned methoxy substituents to the antimigratory and cytotoxic activities of this class. Synthesized analogues were tested in the MTT, cell cycle, and wound-healing assays. Previous studies on this class reported weak to medium antimitotic activity. Therefore, all compounds were subjected to tubulin polymerization assay and in silico molecular docking study at the colchicine binding site of tubulin. The 2-methoxy and 2,4-dimethoxy substitutions at the 2-aryl-pyrimido functionality enhanced the antimigratory activity in the 9-methoxy-substituted series like **6** and **9**. The 3,4,5-trimethoxy substitutions at the 2-arylpyrimido group also significantly improved the antimigratory activity in the presence or absence of the 9-methoxy substitution as represented by **13** and **22**, respectively. Docking experiments showed two distinct orientations at the colchicine binding site of tubulin. The first, achieved by **7** and **16–20**, coincides with that of colchicine and positions the methoxy-substituted 2-aryl ring deep in the highly hydrophobic narrow end of the funnel-shaped binding pocket. On the other hand, **5**, **6**, **9–14** and **21**, were oriented towards the wider opening of the binding pocket. Pyrimido[4,5-c]quinolin-1(2*H*)-ones are promising antimigratory hits with potential for future use to control metastatic breast cancers.

Keywords Anticancer · Cytotoxicity · Methoxy substitution · Pyrimido[4,5-c]quinolin-1(2*H*)-ones · Migration · Tubulin · Wound-healing

K. Metwally (✉)
Department of Medicinal Chemistry, Faculty of Pharmacy, Zagazig University, Sharkeya, Egypt
e-mail: kametwally@hotmail.com

A. Khalil
Pharmaceutical Sciences Section, College of Pharmacy, Qatar University, Doha, Qatar

A. Sallam · K. El Sayed
Department of Basic Pharmaceutical Sciences of College of Pharmacy, University of Louisiana at Monroe, Monroe, LA, USA

H. Pratsinis · D. Kletsas
Laboratory of Cell Proliferation and Ageing, Institute of Biology, National Centre of Scientific Research "Demokritos", Athens, Greece

Introduction

The in vitro cytotoxic activity of pyrimido[4,5-c]quinolin-1(2*H*)-one derivatives was previously reported by our group (Metwally *et al.*, 2007a, b, 2010). This class also exerted several other interesting activities. Related phenylquinazolinone derivatives were patented for use as cardiovascular agents (Hansen, 2010). Some of these derivatives demonstrated activity by causing a ≥20 % increase in ApoA-I mRNA at the μM dose level (Hansen, 2010). Related pyrimido fused acridine derivatives also showed moderate antibacterial and antifungal activities (Patel *et al.*, 2006).

Structure–activity relationship study conducted on the 2,5-diaryl series indicated that methoxy derivatives displayed the highest cytotoxic activity (Metwally *et al.*, 2010). The cytotoxicity of these compounds was attributed in-part to their weak to medium antimitotic activity (Metwally *et al.*, 2007a, b, 2010). Microtubule dynamics are implicated in cell adhesion,

Published online: 12 January 2013

migration, and morphology (Mane and Klobukowski, 2008; Zhu *et al*., 1997; Rowinsky *et al*., 1992; Hayot *et al*., 2002). The use of subtoxic doses of antimitotic agents was found to induce significant antimigratory effects (Hayot *et al*., 2002). Therefore, tubulin inhibitors with optimal potency are hypothesized as potential antimetastatic entities with acceptable therapeutic index and low toxicity profiles. This hypothesis, along with the fact that most known antimitotic agents are rich in methoxy groups (Chart 1), which markedly influence their biological activities (Fitzgerald, 1976; Hu *et al*., 2006; Cushman *et al*., 1991, 1992), have initiated the interest to explore the contribution of diverse-positioned methoxy substituents to the antimigratory and cytotoxic activities of pyrimido[4,5-c]quinolin-1(2*H*)-ones along with accurate in vitro and in silico assessment of their antimitotic activity compared to the known antimitotic colchicine.

Methods and materials

Chemistry

Melting points were determined on a Barnstead Electrothermal 9100 melting point apparatus, and are uncorrected. IR spectra were recorded on a Shimadzu FTIR-8400S spectrophotometer as KBr pellets. ^{1}H NMR spectra were recorded in DMSO-d_6 on a Varian-Mercury 300BB at 300 MHz or on a JEOL Eclipse NMR spectrometer at 400 MHz, while ^{13}C NMR spectra were recorded on a JEOL Eclipse NMR spectrometer at 100 MHz. Chemical shifts were reported as parts per million (ppm) downfield from tetramethylsilane (TMS), and coupling constants (*J*) are given in Hertz (Hz). Elemental analyses (C, H, N) were performed at the Microanalytical Unit, Cairo University, Cairo, Egypt. All compounds were >95 % purity as routinely assessed by ^{1}H NMR and thin-layer chromatography (TLC) on aluminum-backed silica gel plates (E-Merck). All solvents were dried by standard methods. Compounds **1**–**3** (Metwally *et al*., 2007a), **14**, **15**, and **17** were previously reported (Metwally *et al*., 2007a).

The synthetic route of pyrimido[4,5-c]quinolines (**5**–**22**) is illustrated in Scheme 1. The starting 3-aminoquinoline-4-carboxylic acids (**1** and **2**) were obtained following a modified Pfitzinger procedure as previously reported (Metwally *et al*., 2007a, b). Lactonization of acids was achieved by heating with acetic anhydride to give the intermediate 1H-[1,3]oxazino[4,5-c]quinolin-1-ones (**3** and **4**) in 79 and 77 % yields, respectively. Treatment of lactones with the appropriate anilines in the presence of sodium acetate under reflux conditions afforded the target compounds (**5**–**22**) in 34–63 % isolated yields.

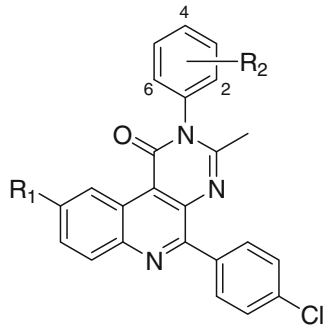

Compound	R_1	R_2	Compound	R_1	R_2
5	OCH_3	H	**14**	H	H
6	OCH_3	2-Methoxy	**15**	H	2-Methoxy
7	OCH_3	3-Methoxy	**16**	H	3-Methoxy
8	OCH_3	4-Methoxy	**17**	H	4-Methoxy
9	OCH_3	2,4-Dimethoxy	**18**	H	2,4-Dimethoxy
10	OCH_3	2,5-Dimethoxy	**19**	H	2,5-Dimethoxy
11	OCH_3	3,4-Dimethoxy	**20**	H	3,4-Dimethoxy
12	OCH_3	3,5-Dimethoxy	**21**	H	3,5-Dimethoxy
13	OCH_3	3,4,5-Trimethoxy	**22**	H	3,4,5-Trimethoxy

*Preparation of 9-methoxy-3-methyl-5-(4-chlorophenyl)-1H-[1,3]oxazino-[4,5-c]quinolin-1-one (**4**)*

A suspension of 3-amino-2-(4-chlorophenyl)-6-methoxy-4-quinolinecarboxylic acid (**2**; 10 mmol) in acetic anhydride (10 mL) was heated at reflux for 5 h. The reaction mixture was allowed to cool to room temperature and the precipitated solid was filtered, washed with EtOH and dried. Yield 77 %, mp 240–242 °C; ^{1}H-NMR (DMSO-d_6) δ: 2.47

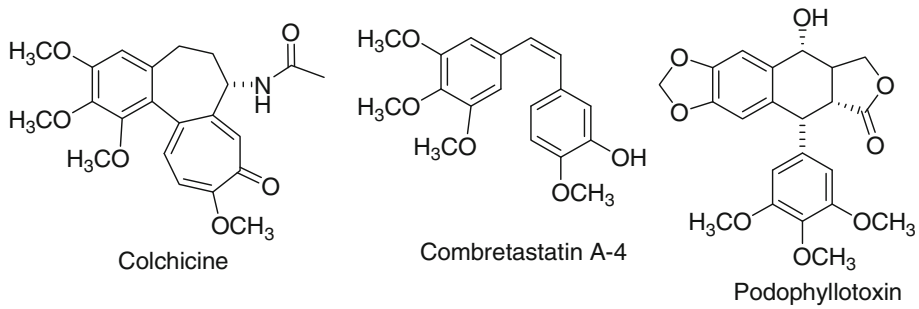

Chart 1 Structure of anti-tubulin agents rich in methoxy groups

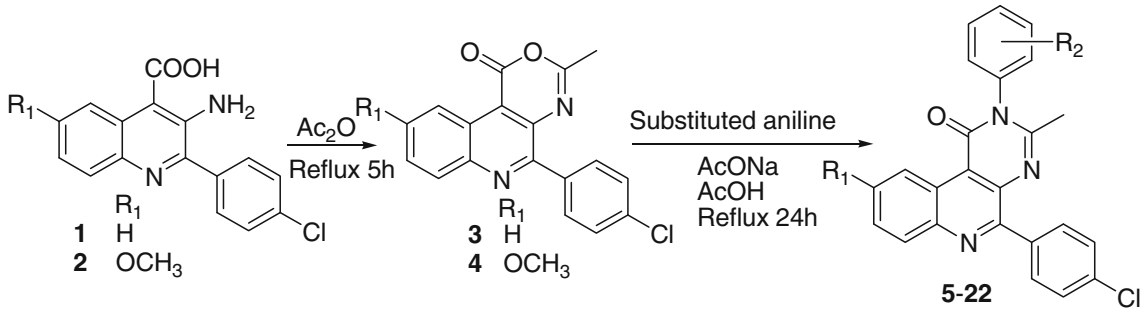

Scheme 1 Synthesis of 3-methyl-2,5-diarylpyrimido[4,5-c]quinolin-1(2H)-ones

(s, 3H, CH_3), 3.96 (s, 3H, OCH_3), 7.52–7.60 (m, 3H, Ar–H), 8.01–8.09 (m, 3H, Ar–H), 8.58–8.59 (d, 1H, $J = 2.8$ Hz, Ar–H). The compound was used without further characterization in the next reactions.

*General procedure for 3-methyl-2,5-diarylpyrimido[4,5-c]quinolin-1(2H)-ones (**5–22**)*

A mixture of the appropriate 1H-[1,3]oxazino[4,5-c]quinolin-1-one (10 mmol), the appropriate substituted aniline (11 mmol) and anhydrous sodium acetate (1.64 g, 20 mmol) in glacial acetic acid (20 mL) was heated under reflux for 24 h. The reaction mixture was cooled, diluted with water (10 mL) and the precipitated solid was filtered, washed with saturated aqueous sodium bicarbonate then water and dried. The crude product was subjected to silica gel column chromatography (using petroleum ether/ethyl acetate (9:1–7:3) as an eluent followed by recrystallization from the appropriate solvent to afford the target compound.

*3-Methyl-9-methoxy-5-(4-chlorophenyl)-2-phenylpyrimido[4,5-c]quinolin-1(2H)-one (**5**)* Yield 62 %, mp 252–254 °C (DMF/EtOH); ^{1}H-NMR (DMSO-d_6): 2.17 (s, 3H, CH_3), 3.88 (s, 3H, OCH_3), 7.42–7.62 (m, 8H, Ar–H), 8.07–8.10 (d, $J = 9.1$ Hz, 1H, Ar–H), 8.13–8.15 (m, 2H, Ar–H), 9.05–9.06 (m, 1H, Ar–H). ^{13}C NMR (DMSO-d_6) δ: 24.99, 55.97, 105.33, 118.75, 121.13, 125.34, 128.14, 128.67, 129.79, 130.32, 131.74, 133.01, 134.00, 137.49, 138.14, 140.60, 141.62, 153.43, 157.08, 159.99, 162.27. Anal. calcd for $C_{25}H_{18}ClN_3O_2$: C, 70.18; H, 4.24; N, 9.82. Found: C, 69.87; H, 4.38; N, 9.71.

*3-Methyl-9-methoxy-5-(4-chlorophenyl)-2-(2-methoxyphenyl)-pyrimido[4,5-c]-quinolin-1(2H)-one (**6**)* Yield 46 %, mp 237–240 °C (DMF); ^{1}H-NMR (DMSO-d_6) δ: 2.19 (s, 3H, CH_3), 3.80 (s, 3H, OCH_3), 3.91 (s, 3H, OCH_3), 7.16–7.21 (m, 1H, Ar–H), 7.31–7.34 (d, $J = 8.35$ Hz, 1H, Ar–H), 7.47–7.51 (m, 2H, Ar–H), 7.54–7.55 (d, $J = 1.6$ Hz, 1H, Ar–H), 7.58–7.61 (m, 2H, Ar–H), 8.09–8.13 (d, $J = 9.1$ Hz, 1H, Ar–H), 8.13–8.18 (m, 2H, Ar–H), 9.05–9.06 (d, $J = 2.9$ Hz, 1H, Ar–H). ^{13}C NMR (DMSO-d_6) δ: 23.98, 55.96, 56.40, 105.41, 113.21, 118.49, 121.11, 121.71, 125.21, 126.05, 128.04, 129.73, 131.58, 131.70, 132.97, 133.96, 137.44, 140.66, 141.58, 153.33, 157.46, 160.07, 161.63, 162.76. Anal. calcd for $C_{26}H_{20}ClN_3O_3$: C, 68.20; H, 4.40; N, 9.18. Found: C, 68.40; H, 4.08; N, 9.10.

*3-Methyl-9-methoxy-5-(4-chlorophenyl)-2-(3-methoxyphenyl)-pyrimido[4,5-c]-quinolin-1(2H)-one (**7**)* Yield 51 %, mp 216–218 °C (DMF/EtOH); ^{1}H-NMR (DMSO-d_6) δ: 2.25 (s, 3H, CH_3), 3.82 (s, 3H, OCH_3), 3.91 (s, 3H, OCH_3), 7.05–7.20 (m, 3H, Ar–H), 7.47–7.51 (dd, $J = 2.9$, 2.9 Hz, 1H, Ar–H), 7.53–7.56 (d, $J = 8.0$ Hz, 1H, Ar–H), 7.58–7.62 (m, 2H, Ar–H), 8.09–8.12 (d, $J = 9.1$ Hz, 1H, Ar–H), 8.14–8.20 (m, 2H, Ar–H), 9.06–9.07 (d, $J = 2.9$ Hz, 1H, Ar–H). ^{13}C NMR (DMSO-d_6) δ: 24.65, 55.92, 55.97, 105.42, 114.34, 115.47, 118.71, 120.59, 120.97, 125.26, 128.05, 130.97, 131.63, 132.93, 133.96, 137.48, 139.16, 140.56, 141.51, 153.25, 156.94, 159.96, 160.80, 162.05. Anal. calcd for $C_{26}H_{20}ClN_3O_3$: C, 68.20; H, 4.40; N, 9.18. Found: C, 68.22; H, 4.18; N, 9.16.

*3-Methyl-9-methoxy-5-(4-chlorophenyl)-2-(4-methoxyphenyl)-pyrimido[4,5-c]-quinolin-1(2H)-one (**8**)* Yield 63 %, mp 209–211 °C (DMF/EtOH); ^{1}H-NMR (DMSO-d_6) δ: 2.22 (s, 3H, CH_3), 3.86 (s, 3H, OCH_3), 3.91 (s, 3H, OCH_3), 7.14–7.18 (m, 2H, Ar–H), 7.41–7.45 (m, 2H, Ar–H), 7.46–7.50 (dd, $J = 2.9$, 2.9 Hz, 1H, Ar–H), 7.58–7.62 (m, 2H, Ar–H), 8.09–8.12 (d, $J = 9.1$ Hz, 1H, Ar–H), 8.15–8.19 (m, 2H, Ar–H), 9.07–9.08 (d, $J = 2.9$ Hz, 1H, Ar–H). ^{13}C NMR (DMSO-d_6) δ: 25.02, 55.95, 56.01, 105.35, 115.41, 118.69, 121.04, 125.35, 128.12, 129.74, 130.57, 131.69, 133.01, 133.99, 137.50, 140.56, 141.55, 153.38, 157.60, 159.96, 160.04, 162.44. Anal. calcd for $C_{26}H_{20}ClN_3O_3$: C, 68.20; H, 4.40; N, 9.18. Found: C, 68.06; H, 4.74; N, 9.07.

*3-Methyl-9-methoxy-5-(4-chlorophenyl)-2-(2,4-dimethoxy-phenyl)-pyrimido [4,5-c]quinolin-1(2H)-one (**9**)* Yield 37 %, mp 243–245 °C (DMF); ^{1}H-NMR (DMSO-d_6) δ:

2.20 (s, 3H, CH_3), 3.78 (s, 3H, OCH_3), 3.88 (s, 3H, OCH_3), 3.92 (s, 3H, OCH_3), 6.72–6.76 (dd, 1H, $J = 2.5$, 2.5 Hz, Ar–H), 6.84–6.85 (d, $J = 2.5$ Hz, 1H, Ar–H), 7.33–7.39 (d, $J = 8.6$ Hz, 1H, Ar–H), 7.45–7.51 (dd, $J = 2.9$, 2.9 Hz, 1H, Ar–H), 7.57–7.61 (m, 2H, Ar–H), 8.09–8.12 (d, $J = 9.1$ Hz, 1H, Ar–H), 8.13–8.18 (m, 2H, Ar–H), 9.06–9.07 (d, $J = 2.8$ Hz, 1H, Ar–H). Anal. calcd for $C_{27}H_{22}ClN_3O_4$: C, 66.46; H, 4.54; N, 8.61. Found: C, 66.80; H, 4.35; N, 8.50.

3-Methyl-9-methoxy-5-(4-chlorophenyl)-2-(2,5-dimethoxyphenyl)-pyrimido[4,5-c] quinolin-1(2H)-one ***(10)*** Yield 41 %, mp 217–219 °C (DMF/EtOH); ^{1}H-NMR (DMSO-d_6) δ: 2.22 (s, 3H, CH_3), 3.74 (s, 3H, OCH_3), 3.77 (s, 3H, OCH_3), 3.91 (s, 3H, OCH_3), 7.12–7.13 (d, 1H, $J = 3.1$ Hz, Ar–H), 7.14–7.15 (m, 1H, Ar–H), 7.23–7.26 (d, $J = 8.8$ Hz, 1H, Ar–H), 7.47–7.51 (dd, $J = 2.9$, 2.9 Hz, 1H, Ar–H), 7.57–7.61 (m, 2H, Ar–H), 8.09–8.12 (d, $J = 9.1$ Hz, 1H, Ar–H), 8.14–8.17 (m, 2H, Ar–H), 9.05–9.06 (d, $J = 2.8$ Hz, 1H, Ar–H). ^{13}C NMR (DMSO-d_6) δ: 24.01, 55.99, 56.23, 56.66, 105.30, 113.93, 115.51, 116.32, 118.52, 121.28, 125.24, 126.40, 128.13, 131.77, 133.02, 134.01, 137.43, 140.67, 141.58, 148.51, 153.42, 154.04, 157.50, 160.08, 161.65. Anal. calcd for $C_{27}H_{22}ClN_3O_4$: C, 66.46; H, 4.54; N, 8.61. Found: C, 66.33; H, 4.73; N, 8.59.

3-Methyl-9-methoxy-5-(4-chlorophenyl)-2-(3,4-dimethoxyphenyl)-pyrimido[4,5-c]quinolin-1(2H)-one ***(11)*** Yield 52 %, mp 223–227 °C (DMF); ^{1}H-NMR (DMSO-d_6) δ: 2.26 (s, 3H, CH_3), 3.78 (s, 3H, OCH_3), 3.86 (s, 3H, OCH_3), 3.91 (s, 3H, OCH_3), 7.02–7.06 (dd, 1H, $J = 2.3$, 2.4 Hz, Ar–H), 7.14–7.18 (m, 2H, Ar–H), 7.46–7.50 (dd, $J = 2.9$, 2.9 Hz, 1H, Ar–H), 7.52–7.62 (m, 2H, Ar–H), 8.05–8.08 (d, $J = 9.1$ Hz, 1H, Ar–H), 8.14–8.19 (m, 2H, Ar–H), 9.08–9.09 (d, $J = 2.9$ Hz, 1H, Ar–H). Anal. calcd for $C_{27}H_{22}ClN_3O_4$: C, 66.46; H, 4.54; N, 8.61. Found: C, 66.34; H, 4.17; N, 8.32.

3-Methyl-9-methoxy-5-(4-chlorophenyl)-2-(3,5-dimethoxyphenyl)-pyrimido[4,5-c]quinolin-1(2H)-one ***(12)*** Yield 55 %, mp 221–224 °C (DMF); ^{1}H-NMR (DMSO-d_6) δ: 2.28 (s, 3H, CH_3), 3.80 (s, 6H, 2 OCH_3), 3.91 (s, 3H, OCH_3), 6.68–6.70 (m, 1H, Ar–H), 6.75–6.76 (d, $J = 2.0$ Hz, 2H, Ar–H), 7.46–7.50 (dd, $J = 2.7$, 2.8 Hz, 1H, Ar–H), 7.56–7.61 (m, 2H, Ar–H), 8.07–8.10 (d, $J = 9.1$ Hz, 1H, Ar–H), 8.14–8.17 (m, 2H, Ar–H), 9.05–9.06 (d, $J = 2.8$ Hz, 1H, Ar–H). Anal. calcd for $C_{27}H_{22}ClN_3O_4$: C, 66.46; H, 4.54; N, 8.61. Found: C, 66.37; H, 4.59; N, 8.69.

3-Methyl-9-methoxy-5-(4-chlorophenyl)-2-(3,4,5-trimethoxyphenyl)-pyrimido[4,5-c]quinolin-1(2H)-one ***(13)*** Yield 57 %, mp 253–256 °C (DMF/EtOH); ^{1}H-NMR (DMSO-d_6) δ: 2.30 (s, 3H, CH_3), 3.77 (s, 3H, OCH_3), 3.80 (s, 6H, 2 OCH_3), 3.92 (s, 3H, OCH_3), 6.93 (s, 2H, Ar–H), 7.47–7.51 (dd, $J = 2.9$, 2.9 Hz, 1H, Ar–H), 7.58–7.62 (m, 2H, Ar–H), 8.09–8.12 (d, $J = 9.1$ Hz, 1H, Ar–H), 8.14–8.18 (m, 2H, Ar–H), 9.08–9.09 (d, $J = 2.9$ Hz, 1H, Ar–H). ^{13}C NMR (DMSO-d_6) δ: 24.68, 56.01, 56.67, 60.64, 105.29, 106.19, 118.73, 121.21, 125.40, 128.17, 128.22, 131.75, 132.96, 132.99, 133.78, 134.00, 137.51, 140.58, 141.56, 154.11, 157.50, 159.97, 162.29. Anal. calcd for $C_{28}H_{24}ClN_3O_5$: C, 64.93; H, 4.67; N, 8.11. Found: C, 65.02; H, 4.38; N, 8.22.

3-Methyl-5-(4-chlorophenyl)-2-(3-methoxyphenyl)-pyrimido[4,5-c]quinolin-1(2H)-one ***(16)*** Yield 59 %, mp 229–231 °C (DMF/EtOH); ^{1}H-NMR (DMSO-d_6) δ: 2.25 (s, 3H, CH_3), 3.82 (s, 3H, OCH_3), 7.08–7.18 (m, 3H, Ar–H), 7.51–7.64 (m, 3H, Ar–H), 7.76–7.89 (m, 2H, Ar–H), 8.15–8.22 (m, 3H, Ar–H), 9.56–9.59 (m, 1H, Ar–H). ^{13}C NMR (DMSO-d_6) δ: 24.79, 55.98, 114.31, 115.50, 119.63, 120.58, 123.82, 126.17, 128.22, 129.52, 129.80, 130.28, 131.08, 133.13, 134.41, 137.35, 139.24, 141.43, 144.70, 156.58, 157.25, 160.79, 161.89. Anal. calcd for $C_{25}H_{18}ClN_3O_2$: C, 70.18; H, 4.24; N, 9.82. Found: C, 70.33; H, 4.07; N, 9.96.

3-Methyl-5-(4-chlorophenyl)-2-(2,4-dimethoxyphenyl)-pyrimido[4,5-c]quinolin-1(2H)-one ***(18)*** Yield 34 %, mp 267–270 °C (DMF); ^{1}H-NMR (DMSO-d_6) δ: 2.20 (s, 3H, CH_3), 3.78 (s, 3H, OCH_3), 3.88 (s, 3H, OCH_3), 6.73–6.76 (dd, 1H, $J = 2.5$, 2.6 Hz, Ar–H), 6.84–6.85 (d, $J = 2.5$ Hz, 1H, Ar–H), 7.36–7.39 (d, $J = 8.6$ Hz, 1H, Ar–H), 7.60–7.64 (m, 2H, Ar–H), 7.76–7.89 (m, 2H, Ar–H), 8.15–8.22 (m, 3H, Ar–H), 9.54–9.58 (dd, $J = 1.4$, 1.1 Hz, 1H, Ar–H). ^{13}C NMR (DMSO-d_6) δ: 24.18, 56.16, 56.53, 100.05, 106.32, 118.86, 119.31, 123.75, 126.16, 128.18, 129.56, 129.84, 130.18, 130.29, 133.18, 134.39, 137.32, 141.44, 144.76, 155.38, 156.64, 158.29, 161.60, 161.86. Anal. calcd for $C_{26}H_{20}ClN_3O_3$: C, 68.20; H, 4.40; N, 9.18. Found: C, 67.96; H, 4.72; N, 9.06.

3-Methyl-5-(4-chlorophenyl)-2-(2,5-dimethoxyphenyl)-pyrimido[4,5-c]quinolin-1(2H)-one ***(19)*** Yield 38 %, mp 225–228 °C (DMF); ^{1}H-NMR (DMSO-d_6) δ: 2.22 (s, 3H, CH_3), 3.74 (s, 3H, OCH_3), 3.77 (s, 3H, OCH_3), 7.12–7.13 (d, 1H, $J = 3.1$ Hz, Ar–H), 7.15–7.17 (m, 1H, Ar–H), 7.24–7.27 (d, $J = 9.2$ Hz, 1H, Ar–H), 7.59–7.64 (m, 2H, Ar–H), 7.77–7.89 (m, 2H, Ar–H), 8.15–8.22 (m, 3H, Ar–H), 9.54–9.57 (dd, $J = 1.2$, 1.7 Hz, 1H, Ar–H). ^{13}C NMR (DMSO-d_6) δ: 24.05, 56.22, 56.72, 114.01, 115.49, 116.32, 119.36, 123.70, 126.16, 126.44, 128.20, 129.60, 129.90, 130.31, 133.17, 134.41, 137.29, 141.44, 144.77, 148.50, 154.04, 156.62, 157.64, 161.32. Anal. calcd for $C_{26}H_{20}ClN_3O_3$: C, 68.20; H, 4.40; N, 9.18. Found: C, 68.09; H, 4.32; N, 9.14.

*3-Methyl-5-(4-chlorophenyl)-2-(3,4-dimethoxyphenyl)-pyrimido[4,5-c]quinolin-1(2H)-one (**20**)* Yield 56 %, mp 245–247 °C (DMF); ^{1}H-NMR (DMSO-d_6) δ: 2.26 (s, 3H, CH_3), 3.77 (s, 3H, OCH_3), 3.86 (s, 3H, OCH_3), 7.02–7.06 (dd, 1H, $J = 2.3$, 2.3 Hz, Ar–H), 7.15 (s, 1H, Ar–H), 7.17–7.18 (d, $J = 2.0$ Hz, 1H, Ar–H), 7.58–7.64 (m, 2H, Ar–H), 7.76–7.89 (m, 2H, Ar–H), 8.16–8.21 (m, 3H, Ar–H), 9.57–9.60 (dd, $J = 1.3$, 1.1 Hz, 1H, Ar–H). ^{13}C NMR (DMSO-d_6) δ: 24.87, 56.22, 56.25, 112.16, 112.46, 119.59, 120.55, 123.85, 126.18, 128.21, 129.48, 129.74, 130.26, 130.67, 133.12, 134.40, 137.37, 141.38, 144.68, 149.60, 149.95, 156.56, 157.89, 162.11. Anal. calcd for $C_{26}H_{20}ClN_3O_3$: C, 68.20; H, 4.40; N, 9.18. Found: C, 68.30; H, 4.37; N, 9.20.

*3-Methyl-5-(4-chlorophenyl)-2-(3,5-dimethoxyphenyl)-pyrimido[4,5-c]quinolin-1(2H)-one (**21**)* Yield 53 %, mp 219-221 °C (DMF); ^{1}H-NMR (DMSO-d_6) δ: 2.33 (s, 3H, CH_3), 3.80 (s, 6H, 2 OCH_3), 6.69–6.70 (m, 1H, Ar–H), 6.75–6.76 (d, $J = 2.0$ Hz, 2H, Ar–H), 7.61–7.63 (dd, $J = 2.0$, 2.0 Hz, 2H, Ar–H), 7.78–7.85 (m, 2H, Ar–H), 8.16–8.20 (m, 3H, Ar–H), 9.56–9.57 (dd, $J = 1.0$, 1.0 Hz, 1H, Ar–H). ^{13}C NMR (DMSO-d_6) δ: 24.45, 56.08, 101.53, 106.84, 119.55, 123.75, 126.10, 128.12, 129.38, 129.67, 130.19, 133.05, 134.36, 137.31, 139.75, 141.32, 144.67, 156.42, 157.11, 161.65, 161.69. Anal. calcd for $C_{26}H_{20}ClN_3O_3$: C, 68.20; H, 4.40; N, 9.18. Found: C, 68.39; H, 4.48; N, 9.31.

*3-Methyl-5-(4-chlorophenyl)-2-(3,4,5-trimethoxyphenyl)-pyrimido[4,5-c]quinolin-1(2H)-one (**22**)* Yield 54 %, mp 240–241 °C (DMF/EtOH); ^{1}H-NMR (DMSO-d_6) δ: 2.31 (s, 3H, CH_3), 3.77 (s, 3H, OCH_3), 3.80 (s, 6H, 2 OCH_3), 6.93 (s, 2H, Ar–H), 7.61–7.64 (d, $J = 8.5$ Hz, 2H, Ar–H), 7.77–7.89 (m, 2H, Ar–H), 8.16–8.22 (m, 3H, Ar–H), 9.58–9.61 (dd, $J = 1.5$, 1.5 Hz, 1H, Ar–H). ^{13}C NMR (DMSO-d_6) δ: 24.67, 56.67, 60.65, 106.18, 119.58, 123.80, 126.16, 128.23, 129.52, 129.79, 130.29, 133.11, 133.74, 134.41, 137.34, 138.11, 141.36, 144.70, 154.10, 156.54, 157.64, 161.92. Anal. calcd for $C_{27}H_{22}ClN_3O_4$: C, 66.46; H, 4.54; N, 8.61. Found: C, 66.70; H, 4.80; N, 8.95.

Biological activity

MTT assay

Compounds **5–22** were tested for their cytotoxic activity on the following human solid tumor cell lines: lung fibrosarcoma HT-1080 (ATCC, Rockville, MD), mammary adenocarcinoma MDA-MB-231 (ATCC), and colorectal adenocarcinoma HT-29 (European Collection of Cell Cultures, Salisbury, U.K.). All cells were routinely cultured in Dulbecco's Minimal Essential Medium (DMEM) supplemented with penicillin (100 IU/mL), streptomycin (100 μg/mL), and 10 % fetal bovine serum (media and antibiotics were from Biochrom KG, Berlin, Germany, while the serum from Invitrogen Co., Carlsbad, CA, USA) in an environment of 5 % CO_2, 85 % humidity, and 37 °C, and they were subcultured using a trypsin 0.25 %-EDTA 0.02 % solution. The cytotoxicity assay was performed by a modification of the MTT method (Metwally *et al.*, 2007a). Briefly, the cells were plated at a density of approximately 5,000 cells/well in 96-well flat-bottomed microplates for 24 h after which individual tested compound stocks were prepared in DMSO and appropriate dilutions were prepared using the assay media and added. After a 72-h incubation, the medium was replaced with MTT (Sigma) dissolved at a final concentration of 1 mg/mL in serum-free, phenol-red-free DMEM and incubated for 4 h. Then, the MTT formazan was solubilized in 2-propanol, and the optical density was measured with a microplate reader at a wavelength of 550 nm (reference wavelength 690 nm). Doxorubicin hydrochloride was included in the experiments as a positive control (Metwally *et al.*, 2007a). The results represent the mean of three independent experiments and are expressed as IC_{50}, the concentration that reduced by 50 % the optical density of treated cells with respect to untreated controls.

Cell cycle analysis

Cell–cycle analysis was performed following incubation of exponentially growing HT-1080 cells with the test substances (2 μM) for 36 h. Treated cultures were then trypsinized, washed in PBS, fixed in 50 % ethanol, and stained with an RNAse-containing propidium iodide solution (Metwally *et al.*, 2007a). For apoptosis assessment through subdiploid event analysis, a DNA extraction step with phosphate-citrate buffer was included prior to flow cytometry (Gong *et al.*, 1994). DNA content was analyzed on a FACS Calibur (Becton–Dickinson, San Jose, CA, USA) flow cytometer using the ModFit software (Verity Software House, Topsham, ME, USA).

Tubulin polymerization assay

The tubulin polymerization assay kit was purchased from Cytoskeleton, Inc. (Denver, CO) and the assay performed as per manufacturer's recommendations (Cytoskeleton Tubulin Polymerization Assay Booklet, Version 8.3). Briefly, 10 μL of each of the controls and test compounds at 100 μM (10× the desired final concentration) in general tubulin buffer (provided with the kit) was added to separate wells of a pre-warmed (37 °C) half area 96-well plate. 100 μL of tubulin solution was then added and the plate immediately transferred to a pre-warmed plate reader. Absorbance was measured at 340 nm and 37 °C every minute for 70 min. The tubulin solution contains 100 μL

volume of 3 mg/mL tubulin in 80 mM pH 6.9, 0.5 mM EGTA, 2 mM $MgCl_2$, 1 mM GTP and 10 % glycerol.

Wound-healing assay

MDA-MB-231 human breast cancer cells were cultured in RPMI 1640 medium containing 10 mM HEPES, 4 mM L-glutamine, 10 % fetal bovine serum, penicillin (100 IU/mL), and streptomycin (50 μg/mL), and incubated in a 5 % CO_2 atmosphere at 37 °C (Sallam *et al*., 2010). Cells were then plated onto sterile 24-well plates and allowed to form a confluent monolayer (>95 % confluence) overnight. Wounds were then inflicted in each cell monolayer using a sterile 200 μL pipette tip. Media was removed and cells were washed twice with PBS and once with fresh serum-free media. Test compounds prepared in serum-free media, from DMSO stock solutions, at the desired concentrations (0.5, 1, 2, 5, 10, 20, 40, 50, and 100 μM) were added to each well. Plates were then incubated for 24–48 h, after which media was removed and cells were washed, fixed and stained using Diff-Quick™ staining (Dade Behring Diagnostics, Aguada, Puerto Rico). Cells which migrated across the inflicted wound were counted under the microscope in three or more randomly selected fields (magnification: ×400). Final results were expressed as percentage mean number of cell for tested compound/mean number of cells for vehicle control ±SEM per ×400 field.

Molecular modeling

Three-dimensional structure building and all modeling were performed using the SYBYL program package, version 8.1, installed on DELL desktop workstations equipped with a dual 2.0 GHz Intel® Xeon® processor running the Red Hat Enterprise Linux (version 5) operating system. Conformations of each compound were generated using Confort™ conformational analysis. Energy minimizations were performed using the Tripos force field with a distance-dependent dielectric and the Powell conjugate gradient algorithm with a convergence criterion of 0.01 kcal/(mol A) (Clark *et al*., 1989). Partial atomic charges were calculated using the semi-empirical AM1 method in MOPAC 6.0 program (Stewart, 1990).

Molecular docking

Surflex-Dock Program version 2.0 interfaced with SYBYL 8.1 was used to dock the compounds in the colchicine binding site of the tubulin–colchicine–soblidotin: stathmin-like domain complex (PDB 3e22) (Abdelbar *et al*., 2010). Surflex-Dock employs an idealized active site ligand (protomol) as a target to generate putative poses of molecules or molecular fragments. These putative poses were scored using the Hammerhead scoring function (Welch *et al*., 1996; Ruppert *et al*., 1997). The 3D structure was taken from the Brookhaven Protein Databank (PDB code: 3e22). To validate each docking experiment, the co-crystallized ligand colchicine was extracted and re-docked. SYBYL successfully and reliably produced the binding mode observed in the crystal structure. The same docking parameters were applied to all compounds and crystallographic colchicine was used as a reference.

Results and discussion

The MTT assay allows for the measurement of cell viability and proliferation of cell populations in a quantitative colorimetric fashion by utilizing cellular ability to reduce the MTT reagent to insoluble purple formazan dye (Sallam *et al*., 2010). Compounds were tested for their cytotoxic activity on the following human solid tumor cell lines: lung fibrosarcoma HT-1080, mammary adenocarcinoma MDA-MB-231 and colorectal adenocarcinoma HT-29. Each compound was tested at five serial dilutions from 100 μM down to 0.16 μM. The concentration of each compound that resulted in 50 % cell growth inhibition, IC_{50}, was calculated (Table 1). With the exception of **13** and **22**, all compounds were not cytotoxic to HT-29 cell line. On the

Table 1 Cytotoxicity of 3-methyl-2,5-diarylpyrimido[4,5-c]quinolin-1(2H)-ones (IC_{50} in μM)

Compound	HT-1080		MDA-MB-231		HT-29	
	Mean	SEM	Mean	SEM	Mean	SEM
5	27.67	9.47	[b]		[b]	
6	10.55	0.18	15.35	0.36	[a]	
7	[a]		[a]		[a]	
8	[a]		[a]		[a]	
9	5.54	0.29	10.68	0.83	[a]	
10	17.13	1.63	51.74	1.78	[a]	
11	97.35	0.94	[a]		[a]	
12	[a]		[a]		[a]	
13	12.71	2.14	16.92	1.17	53.46	6.72
14	13.02	0.30	[b]		[b]	
15	32.34	0.77	44.33	1.02	[a]	
16	38.82	7.10	55.39	3.05	[a]	
17	33.28	9.92	56.8	15.27	[a]	
18	14.13	1.09	44.51	2.29	[a]	
19	19.53	2.40	47.07	0.05	[a]	
20	52.27	2.72	[a]		[a]	
21	76.18	0.94	46.47	1.15	[a]	
22	3.16	0.12	4.45	0.62	68.07	7.27
Doxorubicin	0.02	0.04	0.03	0.02	0.35	0.12

SEM Standard error of the mean

[a] $IC_{50} > 100$ μM, [b] Not tested

other hand, most compounds were moderately active against MDA-MB-231, and HT-1080 cell lines. In general, HT-1080 was the most susceptible among these two cell lines, as previously observed (Metwally *et al.*, 2010). The C-9 methoxy group evidently reduces the cytotoxicity compared to other compounds lacking this group in the same position, except compounds **6** and **9** which showed higher cytotoxicity compared to their respective 9-demethoxy structures **15** and **18**, respectively. This could be justified by reducing the tubulin binding affinity as explained later. Finally, the most active compound against MDA-MB-231 and HT-1080 was **22**, with IC_{50} values 4.45 and 3.16 μM, respectively. Compounds **9**, **6** and **13** were the next most active with IC_{50} range from 5.54 to 16.92 μM (Table 1) against both cell lines.

Cell cycle analysis

Table 2 lists the results obtained with the most promising compounds **6**, **9**, **13**, and **22** administered at a concentration of 20 μM for 48 h versus vehicle control. It is obvious that the most cytotoxic compound **22** showed lowest S-phase, highest G_2/M, together with the lowest IC_{50} value in the cytotoxicity assays. Notably, the microscopic appearance of the cells treated with **22** and to a lesser extent with **13**, was suggesting apoptotic death (i.e. cell shrinkage and detachment). This was supported by the existence of high numbers of subdiploid events during cell cycle analysis, especially when a phosphate-citrate buffer was used for DNA extraction prior to flow cytometry (Gong *et al.*, 1994). In Table 3, a representative experiment showing this induction in the number of subdiploid events during DNA content-analysis by **22**, which was comparable to that produced by the well-known inducer of apoptotic cell death staurosporine (500 μM) (Jarvis and Grant, 1999).

Table 2 Cell cycle phase distribution (%)

Compound	G_0/G_1	S	G_2/M
6	38.7 (±2.6)	26.3 (±0.4)	35.0 (±2.9)
9	40.0 (±3.3)	25.8 (±0.3)	34.2 (±3.1)
13	38.2 (±3.1)	28.0 (±0.6)	33.8 (±2.5)
22	38.7 (±2.4)	17.4 (±0.7)	43.9 (±3.2)
Vehicle control	39.2 (±1.2)	28.1 (±0.5)	32.7 (±1.8)

Average of two experiments

Table 3 Subdiploid events during cell-cycle analysis (%)

Compound	%
22	66.4
Staurosporine	61.5
Vehicle control	13.5

Tubulin polymerization assay

The tubulin polymerization assay kit was used as the in vitro model for the investigation of the effect of **5**–**22** on tubulin polymerization (Fig. 1). In this assay, the extent of tubulin polymerization is proportional to absorbance at 340 nm (Cytoskeleton Tubulin Polymerization Assay Booklet, Version 8.3). Three controls were used, namely DMSO (vehicle control), paclitaxel and colchicine (Chen *et al.*, 2005). All compounds were tested at a single concentration of 10 μM. Table 4 shows the AUC values for tested compounds relative to the vehicle control as % inhibition. It reflects the total amount of tubulin polymer formed per unit time relative to the negative control. AUC values >100 % reflect an increase in tubulin polymerization relative to the negative control, whereas AUC values <100 % are consistent with inhibition of tubulin polymerization. As expected, the AUC value is enhanced by 1.6 fold in the presence of 10 μM paclitaxel, which promotes and stabilizes microtubule polymerization, thus resulting in an overall increase in AUC, and decreased by 4.7 fold in the presence of 10 μM colchicine (a tubulin polymerization inhibitor, thus resulting in an overall decrease in AUC). Generally, all compounds were much less active compared to colchicine. This can be considered as an advantage for future use as cancer migration inhibitors because they may not be as toxic as colchicine. Compounds **6**, **11**, **13**, **17**, **18**, **20** and **21** showed a relatively higher potency compared to other compounds, inducing a decrease in the total amount of polymerized tubulin as reflected by <80 % tubulin polymerization relative to the vehicle control (Table 4). Compound **17**, without C-9-methoxy substitution and with a 4-methoxy substitution on the 2-arylpyrimido ring, shows a tubulin polymerization inhibitory effect comparable to **13**, which has a C-9-methoxy substitution and 3,4,5-trimethoxy on the 2-arylpyrimido substitution. Generally, C-9-methoxy substitution reduced the tubulin polymerization inhibition. 2-Methoxy, 4-methyoxy, 3,4-dimethoxy, 3,5-dimethoxy, or 3,4,5-trimethoxy-2-arylpyrimido substitution pattern was consistent with enhancing the activity (Table 4).

Wound-healing assay

The wound-healing assay is a simple method for the study of directional cell migration in vitro (Rodriguez *et al.*, 2005). Cell migration is relevant to many cellular processes in morphogenesis, tissue repair, as well as cancer invasion and metastasis (Ilina and Friedl, 2009). One of the key steps of cell migration is cytoskeletal rearrangement. The cytoskeleton is a complex, dynamic network consisting of three types of polymers: actin, microtubules, and intermediate filaments (Millipore Product Selection Guide. www.Millipore.com/techpublications/tech1/pb2932en00). There is growing evidence suggesting that microtubules play a

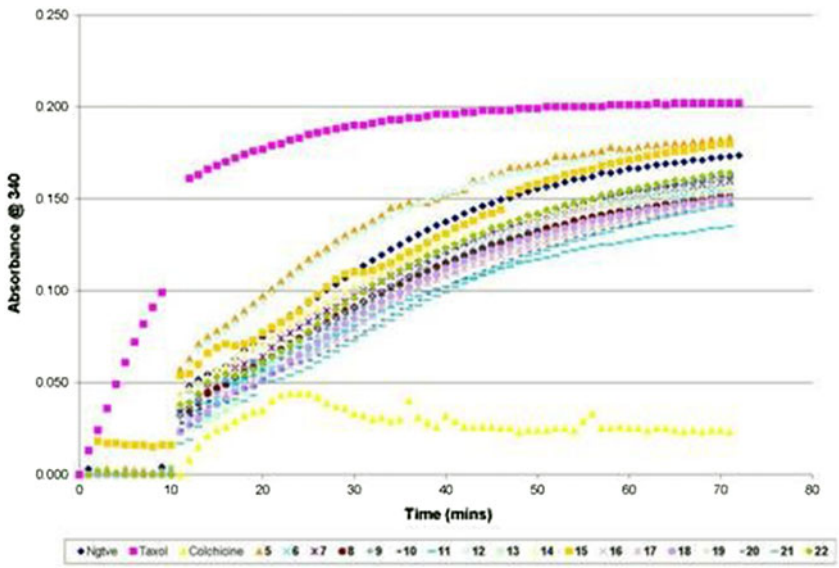

Fig. 1 Tubulin polymerization assay. Purified tubulin at a final concentration of 3 mg/mL was used to assess microtubule formation in vitro in presence of 10 μM doses of test compounds. Changes of absorbance at 340 nm were plotted versus time (minutes)

Table 4 Tubulin polymerization assay and antimigratory activity of 3-methyl-2,5-diarylpyrimido[4,5-c]quinolin-1(2H)-ones in WHA using the human breast cancer cell line, MDA-MB-231

Compound	% Inhibition[a]	Antimigratory IC_{50} (μM)
Vehicle control	100.00	–
Paclitaxel	157.12	–
Colchicine	21.81	7.07
5	107.98	20.84
6	79.79	5.00
7	87.87	23.12
8	83.10	15.58
9	84.49	5.86
10	86.32	8.61
11	74.72	41.51
12	108.74	26.81
13	78.43	2.40
14	90.43	17.98
15	98.73	21.62
16	85.44	20.56
17	77.62	29.42
18	79.90	20.79
19	88.36	14.60
20	75.09	10.17
21	72.91	9.30
22	88.52	1.52

[a] % Inhibition represents the area under the curve for each test compound relative to the vehicle (negative) control

key part in cell polarity and migration through interactions with focal adhesion molecules. Agents affecting microtubule dynamics, such as paclitaxel and nocodazole, also affect cell migration via complex signaling mechanisms (Nakano *et al*., 2010).

Figure 2 shows cell migration across a wound inflicted in an MDA-MB-231 cell monolayer for the vehicle and positive controls. The concentration of each analogue that results in 50 % inhibition of cell migration, IC_{50}, was calculated relative to the vehicle (negative) control using GraphPad Prism 5 (Table 4). The 2-methoxy and 2,4-dimethoxy substitutions at the 2-arylpyrimido functionality enhanced the antimigratory activity in the 9-methoxy-substituted series like **6** and **9** with IC_{50} values of 5.00 and 5.86 μM, respectively. The 3,4,5-trimethoxy substitutions at the 2-arylpyrimido group also significantly improved the antimigratory activity in presence or absence of the 9-methoxy substitution as represented by **13** and **22** with IC_{50} values of 2.40 and 1.52 μM, respectively. The most active compounds in migration assay **6**, **9**, **13**, and **22** were also the most active in the MTT assay but at much lower IC_{50} values, suggesting their activity is not due to direct cytotoxicity. Compound **22**, which is the most active in MTT, cell cycle analysis, and migration assays was among the least active in tubulin polymerization assay with 88.52 % inhibition. This clearly suggests different molecular target for activity other than cytoskeleton.

Molecular modeling and docking studies

Compounds **5**–**22** were docked at the colchicine binding site of the high-resolution crystal structure (resolution = 3.80 Å) of the tubulin–colchicine–soblidotin, stathmin-like domain complex (PDB 3e22) using Surflex-Dock interface implemented into SYBYL 8.1 (Abdelbar *et al*., 2010; Hoshi *et al*., 1996; MacAulay and Woodgett, 2008; Liu and Shen, 2007). Surflex-Dock is a fully automatic flexible molecular docking algorithm that combines the scoring function from the Hammerhead docking system

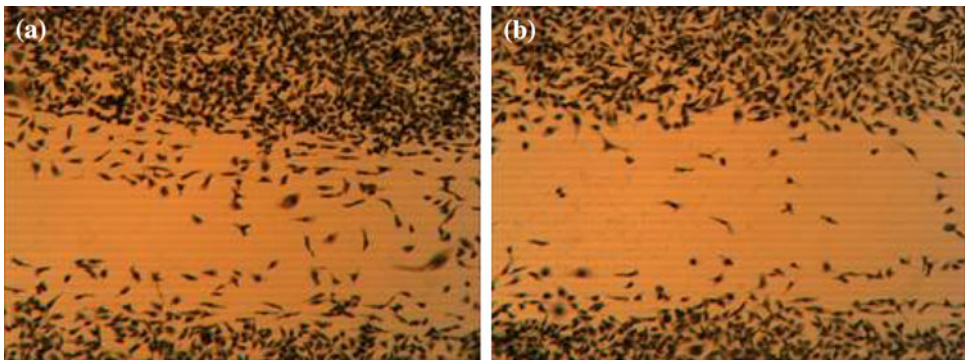

Fig. 2 Graphic Presentation for the WHA using MDA-MB-231 cells after 24 h exposure to: **a** Vehicle (DMSO) treatment as a negative control. **b** A 2 μM dose of the most active compound **22**

with a search engine that relies on a surface-based molecular similarity method as a means to rapidly generate suitable putative poses for molecular fragments (Hoshi *et al.*, 1996; MacAulay and Woodgett, 2008). Three binding domains have been identified in tubulin to date. They include; (*a*) the cholchicine site close to the α/β interface, (*b*) the area where *Vinca* alkaloids binds, and (*c*) the taxane binding pocket. The colchicine binding site lies at the interface between the α- and β-subunits of tubulin, mostly in the β-subunit (Tripathi *et al.*, 2008). The colchicine binding site is a funnel-shaped binding cavity with its narrow part strongly hydrophobic whereas its wider part is moderately polar and hydrophobic (Tripathi *et al.*, 2008). Colchicine is positioned such that its trimethoxy-phenyl moiety fits into the narrow hydrophobic pocket and is surrounded by the amino acids Cys241β, Leu242β, Leu248β, Ala250β, and Leu252β (Fig. 3).

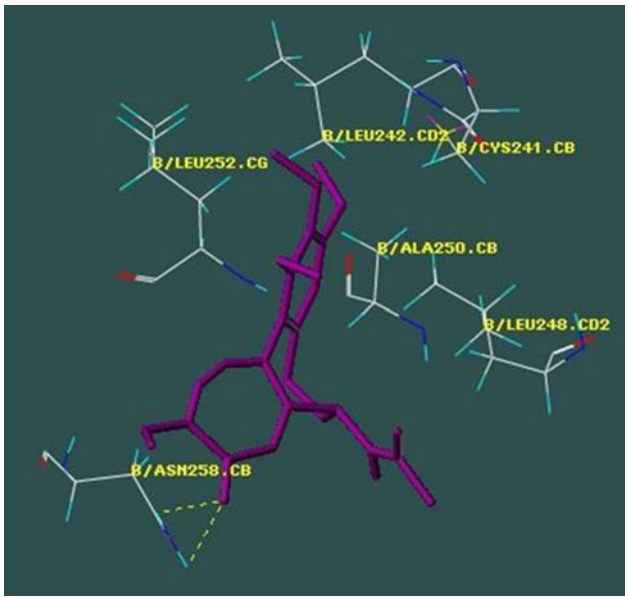

Fig. 3 Detailed view of docked colchicine. Its binding site lies at the interface between the α- and β-subunits of tubulin. Its trimethoxy phenyl moiety fits into the narrow hydrophobic pocket and is surrounded by the amino acids Cys241β, Leu242β, Leu248β, Ala250β, and Leu252β

Docking of compounds **5**–**22** resulted in two general high-scoring orientations (Figs. 4 and 5, Table 5). The first achieved by **7** and **16**–**20** was very closely similar to the binding mode of colchicine (Fig. 4). With the exception of **7**, all compounds showing this colchicine-like orientation lack the C-9-methoxy substitution. The mono- or dimethoxy substituted 2-arylpyrimido ring was deeply embedded in the highly hydrophobic narrow end of the funnel-shaped binding pocket, and was surrounded by Cys241β, Leu242β, Leu248β, Ala250β, Leu255β, Ala354β, and Ileu378β amino acids (Tripathi *et al.*, 2008). Polar interactions also contributed to binding as follows: the oxygen of the 3-methoxy group acts as a hydrogen bond acceptor (HBA) and is located at (3.606–4.093) and (3.752–4.032) Å away from the amide H of the amino acids Cys241β and Leu242β, respectively (Fig. 4 and Table 5). The quinoline nitrogen was also involved in hydrogen bonding and lies within (3.670–3.984) Å of the NH_2 group of Asn258β. Finally, N-4 of the pyrimidine ring was

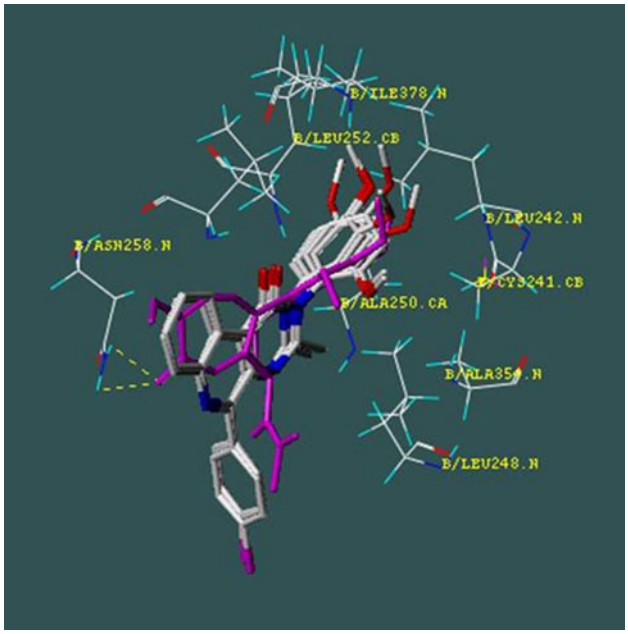

Fig. 4 Detailed view of docked structures **7** and **16**–**20** with a colchicine-like binding mode

involved in hydrogen bonding with the NH_2 group of Asn101β (Fig. 4).

The second orientation was observed for compounds **5**, **6**, **9**–**14** and **21** with a C-9-methoxy substitution along with **14** and **21**, which lack this C-9-methoxy substitution. The oxygen of C-9-methoxy group forms a strong hydrogen bond (2.593–3.207 Å) with the NH_2 group of Lys254β, thus anchoring each molecule in a way that prevented the deep embedding of the methoxy substituted 2-arylpyrimido ring in the narrow hydrophobic pocket (Fig. 5). Instead, each molecule is oriented towards the wider opening of the binding pocket. Compounds **8**, **15** and **22** were exceptions in that they do not fit any of the previously described binding orientations and generally resulted in low docking scores (Fig. 6 and Table 5).

In conclusion, methoxy substitutions on 2-arylpyrimido moieties of Pyrimido[4,5-c]quinolin-1(2*H*)-ones play important role in enhancing their antimigratory activity. The C-9 methoxy substitution significantly reduces the microtubule polymerization inhibitory activity. Generally, all compounds showed reduced tubulin binding affinity compared to

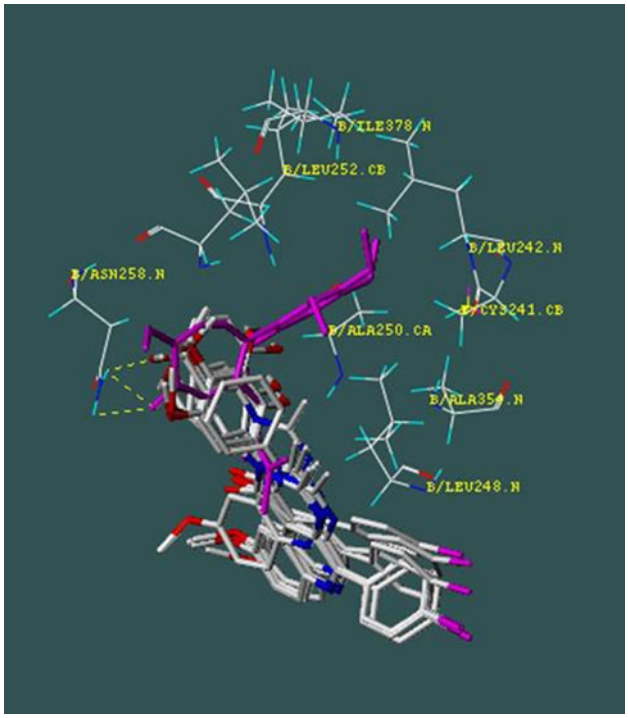

Fig. 5 Detailed view of docked structure for compounds **5**, **6** and **9**–**13**. Their 9-methoxy oxygens form strong hydrogen bond with Lys254β NH_2 group, anchoring each molecule in a way that prevented the deep embedding of the methoxy-substituted 2-phenylpyrimido ring in the narrow hydrophobic pocket

Table 5 Virtual binding affinity of tested compounds at the colchicine binding site of tubulin (PDB 3e22) using SYBYL 8.1 Surflex-Dock

Compound	Docking score	Crash	**Polar**	CScore
Colchicine	7.21	−1.35	0.02	3
5	5.52	−1.67	1.48	4
6	4.97	−2.39	1.00	2
7	5.10	−5.17	0.00	4
8	1.71	−4.74	0.00	4
9	6.39	−2.08	1.22	4
10	3.24	−4.10	0.80	2
11	6.35	−2.16	1.42	4
12	2.16	−5.76	0.08	4
13	5.17	−4.40	1.58	2
14	4.13	−1.62	0.66	1
15	3.65	−2.61	0.00	1
16	5.80	−4.08	0.00	4
17	4.99	−4.85	0.00	2
18	5.30	−4.17	0.00	4
19	3.46	−6.35	0.00	4
20	5.06	−5.13	0.00	2
21	2.09	−4.86	0.76	4
22	2.92	−10.44	2.68	3

Total score was expressed in $-\log(K_d)$ units to represent binding affinities. Crash is the degree of inappropriate penetration by the ligand into the protein and of interpenetration between ligand atoms that are separated by rotatable bonds. Polar score is the contribution of the polar non-hydrogen bonding interactions to the total score. The polar score may be useful for excluding docking results that make no hydrogen bonds

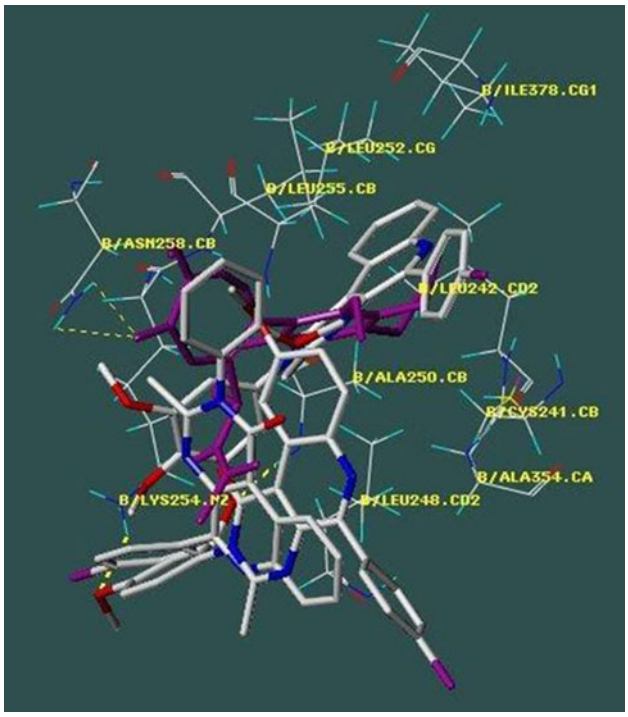

Fig. 6 Docking mode for structures **8**, **15** and **22** versus colchicine

colchicine, which can aid their future use as cancer migration inhibitors because they will not be as toxic as colchicine.

References

Abdelbar F, Khanfar M, Elnagar A, Badria F, Zaghloul A, Ahmad K, Sylvester P, El Sayed K (2010) Design and pharmacophore modeling of biaryl methyl eugenol analogs as breast cancer invasion inhibitors. Bioorg Med Chem 18:496–507

Chen Z, Merta P, Lin N, Tahir S, Kovar P, Sham H, Zhang H (2005) A-432411, a novel indolinone compound that disrupts spindle pole formation and inhibits human cancer cell growth. Mol Cancer Ther 4:562–568

Clark M, Cramer R III, van Opdenbosch N (1989) Validation of the general purpose tripos 5.2 force field. J Comput Chem 10: 982–1012

Cushman M, Magarathnam D, Chakraborti A, Lin C, Hamel E (1991) Synthesis and evaluation of stilbene and dihydrostilbene derivatives as potential anticancer agents that inhibit tubulin polymerization. J Med Chem 34:2579–2588

Cushman M, Magarathnam D, Gopal D, He H, Lin C, Hamel E (1992) Synthesis and evaluation of analogs of (Z)-1-(4-methoxyphenyl)-2-(3,4,5-trimethoxyphenyl)ethene as potential cytotoxic and antimitotic agents. J Med Chem 35:2293–2306

Fltzgerald T (1976) Molecular features of colchicine associated with antimitotic activity and inhibition of tubulin polymerization. Biochem Pharmacol 25:1383–1387

Gong J, Traganos F, Darzynkiewicz Z (1994) A selective procedure for DNA extraction from apoptotic cells applicable for gel electrophoresis and flow cytometry. Anal Biochem 218:314–319

Hansen H (2010) Compounds for the prevention of cardiovascular disease. PCT Int Appl WO 2010079431

Hayot C, Farinelle S, De Decker R, Decaestecker C, Darro F, Kiss R, van Damme M (2002) In vitro pharmacological characterizations of the anti-angiogenic and anti-tumor cell migration properties mediated by microtubule-affecting drugs, with special emphasis on the organization of the actin cytoskeleton. Int J Oncol 21:417–425

Hoshi M, Takashima A, Nogachi K, Murayama M, Sato M, Kondo S, Saitoh Y, Ishiguro K, Hoshino T, Imahori K (1996) Regulation of mitochondrial pyruvate dehydrogenase activity by tau protein kinase I/glycogen synthase kinase 3beta in brain. Proc Natl Acad Sci USA 93:2719–2723

Hu L, Li Z, Li Y, Qu J, Ling Y, Jiang J, Boykin D (2006) Synthesis and structure–activity relationships of carbazole sulfonamides as a novel class of antimitotic agents against solid tumors. J Med Chem 49:6273–6282

Ilina O, Friedl P (2009) Mechanisms of collective cell migration at a glance. J Cell Sci 122:3203–3208

Jarvis W, Grant S (1999) Protein kinase C targeting in antineoplastic treatment strategies. Invest New Drugs 17:227–240

Liu S, Shen Z (2007) A new target for diabetes therapy: advances in the research of glycogen synthase kinase-3 inhibitors. Yaoxue Xuebao 42:1227–1231

MacAulay K, Woodgett J (2008) Targeting glycogen synthase kinase-3 (GSK-3) in the treatment of Type 2 diabetes. Expert Opin Ther Targets 12:1265–1274

Mane J, Klobukowski M (2008) Free energy calculations on the binding of colchicine and its derivatives with the α/β-tubulin isoforms. J Chem Inf Model 48:1824–1832

Metwally K, Pratsinis H, Kletsas D (2007a) Pyrimido[4,5-c]quinolin-1(2H)-ones as a novel class of antimitotic agents: synthesis and in vitro cytotoxic activity. Eur J Med Chem 42:344–350

Metwally K, Aly O, Aly E, Banerjee A, Ravindra R, Bane S (2007b) Synthesis and biological activity of 2,5-diaryl-3-methylpyrimido[4,5-c]quinolin-1(2H)-one derivatives. Bioorg Med Chem 15:2434–2440

Metwally K, Khalil A, Pratsinis H, Kletsas D (2010) Synthesis, in vitro cytotoxicity, and a preliminary structure-activity relationship investigation of pyrimido[4,5-c]quinoline-1(2H)-ones. Arch Pharm Chem Life Sci 8:465–472

Nakano A, Kato H, Watanabe T, Min K, Yamazaki S, Asano Y, Seguchi O, Higo S, Shintani Y, Asanuma H, Asakura M, Minamino T, Kaibuchi K, Mochizuki N, Kitukaze M, Takashima S (2010) AMPK controls the speed of microtubule polymerization and directional cell migration through CLIP-170 phosphorylation. Nat Cell Biol 12:583–593

Patel B, Patel R, Patel M (2006) Synthesis and studies of the biological activity of novel pyrimido fused acridine derivatives. J Serb Chem Soc 71:1015–1023

Rodriguez L, Wu X, Guand J (2005) Wound-healing assay. Methods Mol Biol 294:23–29

Rowinsky E, Onetto N, Canetta R, Arbuck S (1992) Taxol: the first of the taxanes, an important new class of antitumor agents. Seminars Oncol 19:646–662

Ruppert J, Welch W, Jain A (1997) Automatic identification and representation of protein binding sites for molecular docking. Protein Sci 6:524–533

Sallam A, Ramasahayam S, Meyer S, El Sayed K (2010) Design, synthesis, and biological evaluation of dibromotyrosine analogues inspired by marine natural products as inhibitors of human prostate cancer proliferation, invasion, and migration. Bioorg Med Chem 18:7446–7457

Stewart JPP (1990) MOPAC: a semiempirical molecular orbital program. J Comput Aided Mol Des 4:1–105

Tripathi A, Fornabaio M, Kellogg G, Gupton J, Gewirtz D, Yeudall W, Vega N, Mooberry S (2008) Docking and hydropathic scoring of polysubstituted pyrrole compounds with antitubulin activity. Bioorg Med Chem 16:2235–2242

Welch W, Ruppert J, Jain A (1996) Hammerhead: fast, fully automated docking of flexible ligands to protein binding sites. Chem Biol 3:449–462

Zhu Q, Guo Z, Huang N, Wang M, Chu F (1997) Comparative molecular field analysis of a series of paclitaxel analogs. J Med Chem 40:4319–4328